ENTRY FLASHES OF COMETARY FRAGMENTS IN JOVIAN UPPER ATMOSPHERE

S. TAKEUCHI
National Space Development Agency of Japan
Sengen, Tsukuba, Ibaraki 305, Japan

H. HASEGAWA
ASTEC, Inc.
Minami-cho, Shinjuku, Tokyo 162, Japan

AND

J. WATANABE
National Astronomical Observatory of Japan
Osawa, Mitaka, Tokyo 181, Japan

1. Introduction

Short lasting flashes, called as First Precursor (PC1), were observed by some ground-based near-infrared observations for the impacts of large-sized fragments of comet Shoemaker-Levy 9 (SL9) in July 1994. The impact detections by the spacecraft *Galileo* [2, 7] about 10 seconds after the PC1 detections by ground based telescopes, combined with the far-side impacts of SL9 fragments as viewed from Earth, suggest that the source of the PC1 should be located in the Jovian upper atmosphere above the limb, at which the atmospheric pressure is extremely low. Thus, an important problem on the PC1 is how does the falling cometary fragment, which is a huge meteorite, emit near-infrared in the extremely thin atmosphere. The ablation model, which is usually used for an impact bolide, can only estimate flux from the bolide in a dense atmosphere at visible wavelength. In this paper, we assume that the PC1s are thermal radiation from the fragments and attempt quantitative estimations of the PC1 fluxes using a simple entry flash model.

2. Observations of the PC1

A summary of the PC1 observations is given by Table 1. The precise position of impact site for each fragment is an important parameter and determines a minimum height of the fragment seen from Earth direction. We use the impact site estimations by Chodas and Yeomans [3], whose

TABLE 1. Summary of PC1 Observations and Geometry

Frag-ment	Class [5]	PC1 Peak Flux ($Wm^{-2}\mu m^{-1}$/Jy)	Wavelength (μm) / Observatory	Meridian Angle(deg) [3]	Minimum Visible Height above 1bar(km)
A	2a	$9.0 \times 10^{-16}/0.0016$	2.3 / Calar Alto [6]	65.4	556
G	1	$1.8 \times 10^{-14}/0.0048$	0.89/ HST [5]	67.1	410
		$> 5.4 \times 10^{-14}/0.010$	2.34/ CASPIR [8]		
H	2a	$7.9 \times 10^{-14}/0.14$	2.3 / Calar Alto [6]	67.5	367
K	1	$3.0 \times 10^{-13}/0.55$	2.35/ Okayama [12]	68.3	304
L	1	$2.0 \times 10^{-13}/0.36$	2.3 / Calar Alto [6]	68.9	250
Q1	2b	$2.5 \times 10^{-14}/0.045$	2.3 / Calar Alto [6]	69.9	190
R	2b	$2.4 \times 10^{-13}/0.43$	2.3 / Keck [4]	70.2	169
W	2c	$6.0 \times 10^{-13}/0.060$	0.55/ HST [5]	71.2	117

J. Andersen (ed.), Highlights of Astronomy, Volume 11A, 266–269.

meridian angle from the mid-night longitude are shown at 5th column in Table 1, and calculate the minimum visible heights of the fragments. The accuracies of the meridian angles are about 0.1 degree (Chodas, personal communication), which corresponds to the uncertainty of the minimum visible height about some ten kilometers.

3. Entry Flash Model in the Upper Atmosphere

Because the PC1 emission was thermal continuum for AAT observation [9], we must know the temperature of PC1 radiative source in order to estimate the PC1 infrared flux. We assume simply that all the lost energy of the fragment due to the atmospheric drag is radiated from the surface of the fragment, so that we can estimate the radiative temperature using the following formulation.

The equations of motion and energy of the entry fragments are as follows;

$$\frac{du}{dt} = -\frac{C_d}{2m} A\rho V u \,, \tag{1}$$

$$\frac{dw}{dt} = -\frac{C_d}{2m} A\rho V w - g \,, \tag{2}$$

$$\frac{dE}{dt} = -\frac{C_d}{2} A\rho V^3 \,, \tag{3}$$

where u and w are the horizontal and vertical velocity of fragment, V is the speed of fragment ($V^2{=}u^2{+}w^2$), A is the cross section of fragment ($A{=}\pi\ r^2$), r is the radius of fragment, m is the mass of fragment, E is the energy of fragment ($E{=}mV^2/2{+}mgz$), g is the acceleration due to the Jovian gravity (25 m/s^2), z is the altitude above the 1 bar level, ρ is the density of the Jovian atmosphere, C_d is the drag coefficient (1.2). It is assumed that all the lost energy of the fragment due to the atmospheric drag is radiated instantaneously as thermal emission;

$$-\frac{dE}{dt} = (4\pi r^2)\sigma T^4 \,, \tag{4}$$

where σ is Stephan-Boltzmann constant, T is the radiative temperature or the surface temperature of the fragment. From the equations (3) and (4),

$$T = \left(\frac{C_d \rho V^3}{8\sigma}\right)^{1/4} . \tag{5}$$

The flux at wavelength λ, observed at Earth is

$$F_\lambda = B_\lambda(T)\, A\, \frac{1}{\Delta^2} \,, \tag{6}$$

where F_λ is the thermal flux of the fragment at wavelength λ, $B_\lambda(T)$ is the Planck function, Δ is the distance between Jupiter and Earth, which was 5.17AU (7.75×10^8km) at the SL9 impact days, July 1994.

Thus, given the density distribution of the Jovian atmosphere, the flux from a fragment with radius r can be calculated. V is about 60 km sec^{-1}.

4. Jovian atmosphere

We use two different models of the Jovian atmosphere. One is the distribution by Atreya et al. [1], which is called in general as the 'Orton' model. This model has a constant increment of temperature in the thermosphere (above 400 km). Another is the distribution sounded by the *Galileo* probe [10]. This model, called as the 'Probe' model in this paper, shows rapid increment of temperature around the mesopause (350–400 km) and constant, high temperature of 800 K in the thermosphere. But, below the height of 400 km, both atmospheric models have almost same distribution.

These two models are constructed for the Jovian equatorial latitude. Because the SL9 fragments impacted at the mid-latitude of Jupiter, we reconstruct the atmospheric models for the mid-latitude taking into account the difference between the surface gravities of the two latitudes. The vertical distributions of the temperature, the pressure and the density for both models are shown by Fig. 1.

Using the distributions of both models, the entry fluxes of fragments are calculated from equations (5) and (6). Fig. 2 shows the entry fluxes of $2.3\mu m$ for fragments with radii of 1 km, 500 m, and 200 m in the 'Orton' and 'Probe' models.

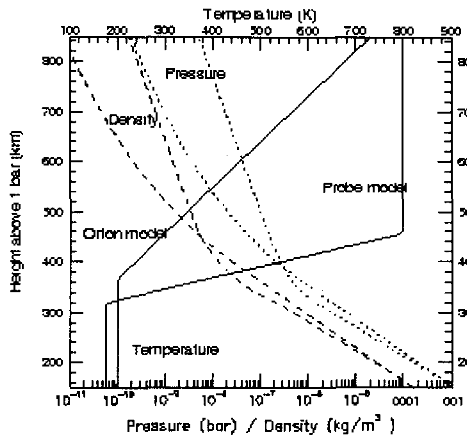

Figure 1. Vertical distributions of temperature (solid lines), pressure (dotted lines), and density (dashed lines) in the Jovian upper atmosphere. Higher values of the temperature, the pressure and the density show the distributions of the Probe model. Lower values show those of the Orton model.

5. Discussion and Summary

First, considering the uncertainty of the minimum visible height, Fig. 2 shows that the fragments H, K, and L, which are known to be the largest ones among the SL9 fragments, have radii of several hundred meters. Some estimations of the fragment sizes (e.g., Sekanina [11]) indicate that the diameters of the largest fragments are about 1 km or less and that the diameters of the medium sized fragments are a few hundred meters, which are consistent with the size estimations derived from the PC1 flux calculation in this paper. The visible ($0.89\mu m$) PC1 flux of the G impact can be also explained by the entry flash model and a fragment with a radius of several hundred meters, in spite of no figure of the result because of lack of space.

Next, we shall take into account three factors, refraction and methane absorption of the Jovian atmosphere and additional flux contributed from dust around the fragment nucleus, which are not incorporated in the entry flash model. The refraction of the atmosphere will decrease the minimum visible height some tens kilometers, but the methane absorption will take the "limb" of Jupiter up to higher altitude than the 1 bar level and will increase the minimum visible height by several tens of kilometers. Thus, these two factors have little effect for the PC1 flux calculation for now.

Also we don't think that the dust around the fragment nucleus has a large contribution to the PC1 flux, because of the weak PC1 flux of fragment Q_1. Q_1 was the brightest fragment among the 22 SL9 fragments [13], which means that there was a large amount of dust around the Q_1 fragment. However, the main event of the Q_1 impact was not largest and the size of the debris cloud after the Q_1 impact was a medium class (2b) [6, 5]. This suggests that the main event and the debris cloud depend on the fragment nucleus, and that the fragment Q_1 consists of a medium size nucleus and a lot of dust around the nucleus. Fig. 2 shows that the PC1 flux of the Q_1 is weak and that the size of the fragment Q_1 is 100 m or less. This is consistent with the suggestion by the main event and the debris, not with the pre-impact brightness, which means that the dust did not contribute to the PC1.

Last, we discuss the PC1 of the A impact, whose minimum visible height is so high that the difference between the two atmospheric models is important. For the Orton model, the estimated

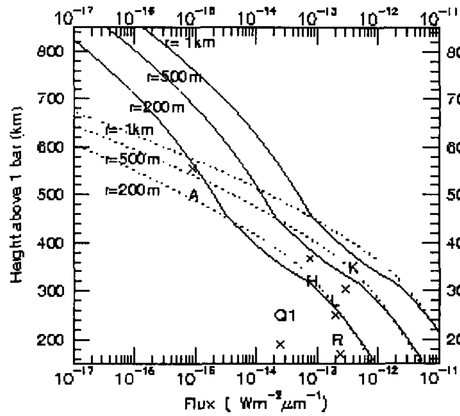

Figure 2. Entry fluxes at the near infrared of 2.3μm in the two atmospheric models. r is the radius of fragment. Solid lines show these fluxes for the Probe model, and dotted lines show those for the Orton model. Crosses are plotted for the observed PC1 fluxes and the minimum visible heights of the fragments.

radius of fragment A is larger than those of fragments H, K, and L. The probe model, on the other hand, indicates that fragment A is of medium class. Because fragment A appears to be of medium size, the probe model is relevant to the thermospheric model of Jupiter.

We conclude that the PC1 is the thermal radiation from the entry fragment due to the atmospheric drag. Also, the PC1 of fragment A, if the A fragment is a medium sized fragment with a radius of one or a few hundred meters, suggests that the Jovian thermosphere must be hot in the mid-latitude like in the equatorial latitude probed by the *Galileo* probe.

References

1. Atreya, S.K., et al. (1981), Jupiter: Structure and composition of the upper atmosphere, *ApJ*, **247**, L43–L47.
2. Chapman, C.R., et al. (1995), Preliminary results of Galileo direct imaging of SL-9 impacts, *GRL*, **22**, pp. 1561–1564.
3. Chodas, P.W., and Yeomans, D.K. (1996), The orbital motion and impact circumstances of Comet Shoemaker-Levy 9, in *The Collision of Comet Shoemaker-Levy 9 and Jupiter*, pp. 1–30, Cambridge University Press.
4. Graham, J.R., et al. (1995), The fragment R collision: W.M.Keck telescope observations of SL9, *Science*, **267**, pp. 1320–1323.
5. Hammel, H., et al. (1995), HST imaging of atmospheric phenomena created by the impact of comet Shoemaker-Levy 9, *Science*, **267**, pp. 1288–1296.
6. Herbst, T.M., et al. (1995), Near infrared imaging and spectroscopy of the SL9 impacts from Calar Alto, *GRL*, **22**, pp. 2413–2416.: Hamilton, D.P., et al. (1995), Calar Alto observations of the Shoemaker-Levy 9: Characteristics of the H and L impacts, *GRL*, **22**, pp. 2417-2420.
7. Martin, T.Z., et al. (1995), Observation of Shoemaker-Levy impacts by the Galileo Photopolarimeter Radiometer, *Science*, **268**, pp. 1875–18798.
8. McGregor, P.J., et al. (1996), CASPIR observations of the collision of comet Shoemaker-Levy 9 with Jupiter, *Icarus*, **121**, pp. 361–388.
9. Meadows, V., and Crisp, D. (1995), Impact plume composition from near-infrared spectroscopy, *Proceedings of European SL9/Jupiter Workshop*, pp. 239–244.
10. Seiff, A., et al. (1996), Structure of the atmosphere of Jupiter: Galileo probe measurements, *Science*, **272**, pp. 844–845.: Seiff, A., et al. (1997), Thermal structure of Jupiter's upper atmosphere derived from the Galileo probe, *Science*, **276**, pp. 102–104.
11. Sekanina, Z. (1996), Collision of comet Shoemaker-Levy 9 with Jupiter: impact study of two fragments from the timing of precursor events, *A&Ap*, **314**, pp. 315–327.
12. Takeuchi, S., et al. (1995), Near-IR imaging observations of the cometary impact into Jupiter, *GRL*, **22**, pp. 1581–1584.
13. Weaver, H.A., et al. (1995), The Hubble Space Telescope (HST) observing campaign on comet Shoemaker-Levy 9, *Science*, **267**, pp. 1282–1288.